

# FATIGUE FRACTURE BEHAVIOUR OF CONCRETE THROUGH WEDGE-SPLITTING TESTS

Srinithya A<sup>\*</sup>, Yogesh R<sup>†</sup> and J M Chandra Kishen<sup>‡</sup>

Department of Civil Engineering, Indian Institute of Science,  
Bangalore, India 560012.

\* e-mail: [srinithyaa@iisc.ac.in](mailto:srinithyaa@iisc.ac.in)

† e-mail: [yogeshr@iisc.ac.in](mailto:yogeshr@iisc.ac.in)

‡ e-mail: [chandrak@iisc.ac.in](mailto:chandrak@iisc.ac.in)

**Key words:** Fracture, Fatigue, Wedge splitting test, Constant Amplitude Fatigue Loading, Acoustic Emission (AE), Micro cracking, Fracture Process Zone (FPZ).

**Abstract.** Fracture in concrete takes place at pre-existing crack tip when a fracture process zone (FPZ) with a number of toughening mechanisms is formed. In order to continually monitor and gain insight into the progression of cracks and its behaviour in concrete, notched wedge-splitting specimens are experimentally investigated under crack opening to examine the fracture and fatigue behaviour of plain concrete when subjected to constant amplitude fatigue loading with a frequency of 1 Hz. The specimens are monitored using acoustic emission (AE) piezo electric sensors to study the rate of crack initiation and growth. Different AE parameters that include events, energy and rise angle are analysed to study the mechanism of microcrack growth under fatigue loading.

## 1 INTRODUCTION

Concrete, a material widely used in construction, is vulnerable to cracking and failure, from a number of sources, including overloading, fatigue, prolonged exposure to extreme conditions and ageing. The term "concrete fracture" describes the splitting or cracking of concrete under stress. Understanding the origins and mechanisms of fracture is crucial for predicting the severity and type of cracks in concrete. During fracture of concrete, inelastic deformation and microcracking take place in the region surrounding the crack which is known as the fracture process zone (FPZ). Numerous toughening processes, including microcracking, aggregate bridging, crack branching, etc., occur in this zone, which dissipates energy and prevents further major crack propagation. Another factor that needs to be given serious con-

sideration is fatigue. When concrete undergoes repeated stress cycles, such as those encountered by bridges, and other structures that are subjected to oscillatory loads from wind, earthquakes, and traffic, fatigue can develop. The existence of internal defects and microscale cracks prior to any load being applied complicates the process of fatigue damage further. Small or micro cracks begin to form and advance over time as a result of the repetitive stress, finally resulting in the full collapse of the concrete structure. Contrary to more uniform and ductile materials like steel, the fatigue behaviour of concrete is not well understood.

To explore the behaviour of concrete subjected to flexural fatigue loading, many researchers [1, 3, 5, 7, 8] have performed experiments on notched concrete beams in a three-point bending arrangement. Several re-

searchers [2,4,6] have experimented with fiber-reinforced concrete, ultra-high strength concrete, and other materials using wedge splitting specimens. Singh et al. [9] conducted research on the mechanism of fracture process in plain concrete under crack opening on wedge splitting specimens. In the current research, the application of constant amplitude fatigue loading on notched wedge splitting specimens with the aid of acoustic emission sensors is used to explore the underlying processes of propagation of cracks and fracture processes in plain concrete.

## 2 EXPERIMENTAL PROGRAM

The experimental program detailing the test procedure, materials used for specimen preparation and the experimental set-up are described in this section.

### 2.1 Test procedure

The fracture properties of plain concrete are obtained from wedge splitting compact tension specimens. The geometry of the wedge splitting specimen is shown in Figure 1. The specimens have uniform thickness of 100 mm.

As illustrated in Figure 2, the cast samples are tested under constant amplitude fatigue loading with sinusoidal oscillations of 1 Hz frequency. In order to ensure proper contact between the loading device and the test sample, the minimum machine load amplitude is kept at 0.4 kN. Based on the results of the monotonic test performed earlier [9], the maximum load amplitude is set at 0.8 times the peak load amplitude. A data acquisition system is used to collect real-time data for load, crack mouth opening displacement (CMOD) simultaneously.

The AE technique is used to record the micro crack progression and evolution. Six piezoelectric sensors are used to collect the AE data,

three of which are placed on the front face and the rest placed behind. The AE sensors have a height of 22 mm, a diameter of 19 mm, and a frequency range of 35 to 100 kHz. As a couplant, high vacuum silicon grease is employed. The AE signals are amplified by preamplifiers with a gain of 40 dB. The AE data has been acquired using an eight-channel AE-WIN for SAMOS E2.0 (Sensor based Acoustic Multi-channel Operating System), built by Physical Acoustics Corporation (PAC)-USA. A 35 dB threshold, which is often utilised for concrete, is chosen. During the investigations, the AE data, including hits, events, energy, absolute energy, signal intensity, spatial coordinates, amplitude, and time, are continuously collected using a data acquisition system. Figure 3 depicts the sample with AE sensors and pre-amplifiers.

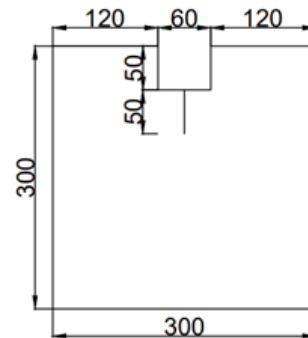


Figure 1: Dimensions of wedge splitting specimens.

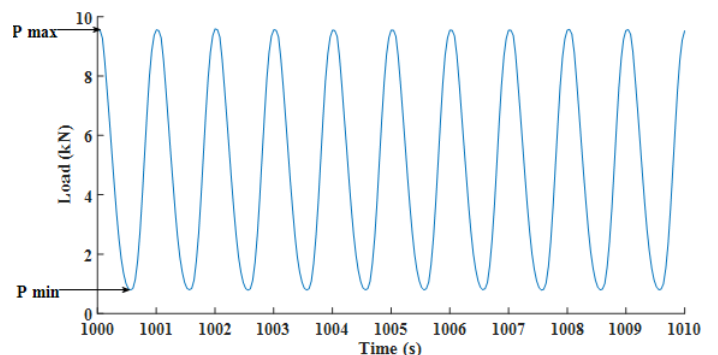


Figure 2: Constant amplitude fatigue loading pattern.

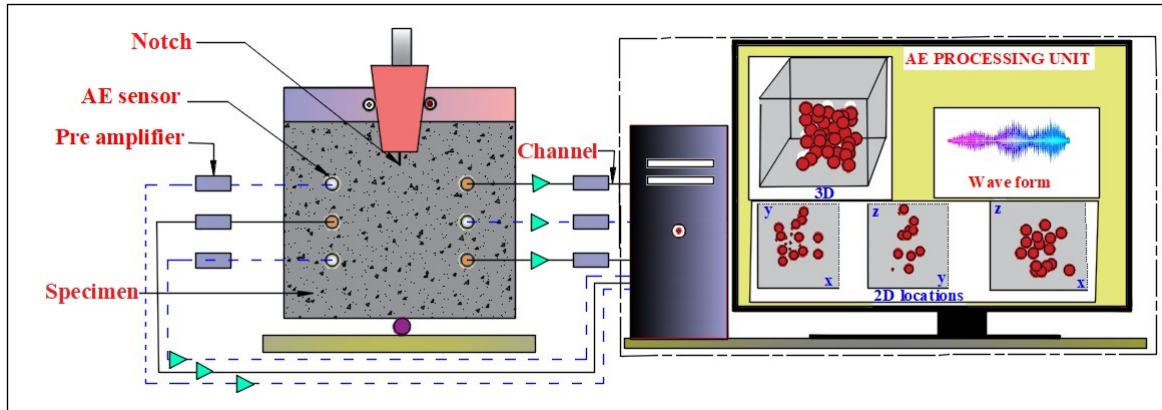


Figure 3: Details of AE system in the specimen.

## 2.2 Materials and preparation of test specimens

Portland pozzolana cement that conforms with IS 1489 part 1 [1991], river sand that is contained within zone III as defined by IS 2386 part 1 [1963], and crushed granite coarse aggregates with a maximum size of 12.5 mm are used to cast the concrete samples. In accordance with IS 10262-2019, the cement, fine aggregate, and coarse aggregate mix proportions were calculated as 1:2.30:2.70 by weight. The concrete is casted with a water to cement ratio of 0.55. By pouring concrete into wooden moulds, the samples are prepared. For creating a notch in the sample, during casting, a 2 mm thick steel plate is placed in the wooden mould. Every sample undergoes a 28-day curing process in a water tank.

## 2.3 Experimental Setup

A digitally controlled closed loop servo-hydraulic universal testing machine with a 35 kN capacity is used to test the samples. Steel plates are fastened across the notch on both sides in order to place a clip gauge that measures CMOD. As shown in Figure 4, the wedge splitting fittings are mounted on the sample. Under the load cell, yet another fixture is attached to the machine's fixed upper crosshead. The samples are held in place at the bottom centre through a roller support. Figure 5 depicts the

experimental setup and a schematic depiction of the sample used during testing.

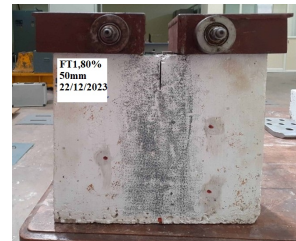


Figure 4: Fixtures of the wedge splitting specimen.

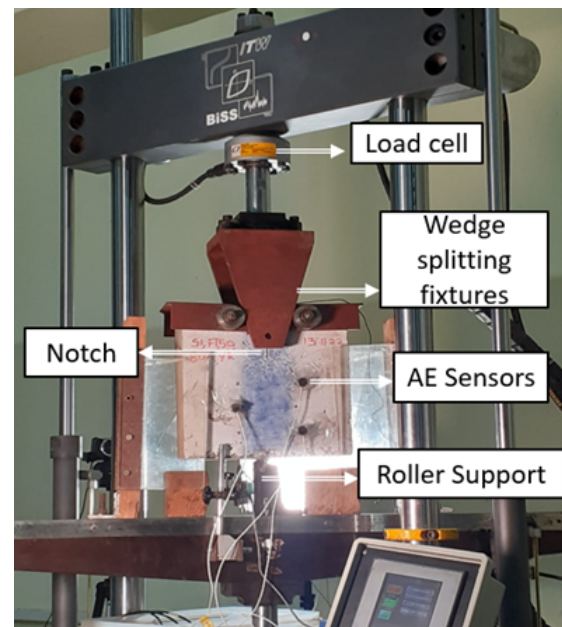


Figure 5: Experimental setup of wedge splitting test.

### 3 RESULTS AND DISCUSSIONS

In this section, results of mechanical and acoustic emission data are presented for the experiments conducted.

#### 3.1 Mechanical results

The major purpose of the wedge splitting constant amplitude fatigue tests used in this study is to examine the fatigue response under splitting tensile load for a particular notch size. Testing is performed using four specimens with 50mm notch size under constant amplitude fatigue loading. The load values indicated in this study are the splitting load in the horizontal direction. The average peak splitting load obtained from monotonic tests is 12.07kN. 80% of the average peak splitting load is applied to the specimens to perform constant amplitude fatigue loading. Table 1 lists the results of all fatigue tests conducted, including the maximum and minimum splitting load amplitudes, cycles to failure and maximum CMOD value at the time of failure. As can be observed from the load versus CMOD plot in Figure 6, the slope of the load versus CMOD curve continuously decreases as the number of loading cycles increases. The stiffness can be calculated from the slope of the load-CMOD curve. Due to ongoing damage occurring inside the specimen as a result of fatigue loading cycles, it is noted that stiffness is gradually declining.

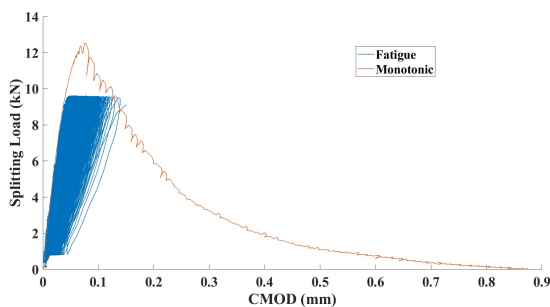
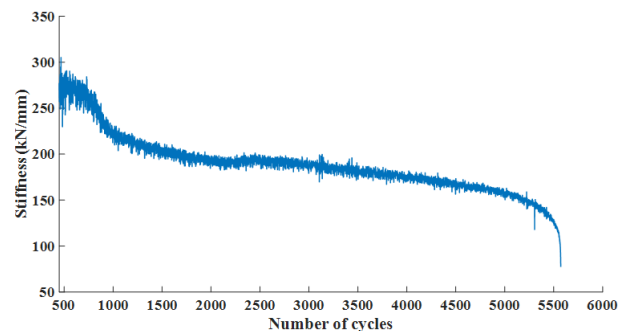


**Figure 6:** Load-CMOD curve (Monotonic & Fatigue).

**Table 1:** Mechanical test results for fatigue loading

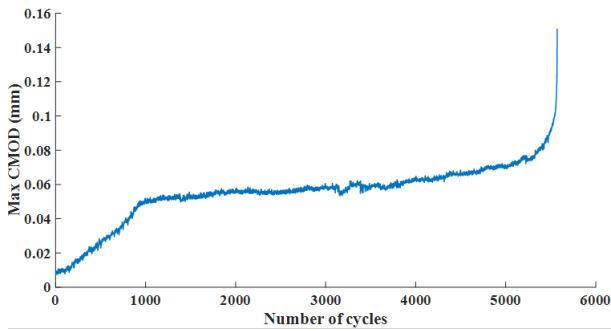
ID	$P_{min}$ (kN)	$P_{max}$ (kN)	Number of cycles to failure ( $N_f$ )	Maximum CMOD at failure (mm)
A1	0.74	9.658	2173	0.416
A2	0.74	9.658	1330	0.203
A3	0.74	9.658	5581	0.151
A4	0.74	9.658	1392	0.247

Figure 7 depicts a stiffness vs number of cycles curve for the A3 specimen. As the number of loading cycles increases, it is observed that stiffness steadily decreases. As the specimen is loaded during the initial loading phase, a sudden drop in stiffness is seen. This is related to the development of internal microcracks as the load is applied, which may be caused by stress concentration at the voids and flaws of the intact sample. These micro cracks are scattered randomly across the specimen's entire volume and are isolated. After redistribution of stresses that occur in the initial loading phase, the rate of stiffness deterioration is nearly constant for majority of the fatigue life, suggesting that a stable crack propagation is occurring inside the specimen. Numerous microcracks form at this phase, although the pace at which damage develops remains essentially constant. The stiffness abruptly falls at the final stage of the fatigue life, at which point the microcracks combine to form a large crack that causes failure. Here, it is seen that the specimen loses up to 50% of its initial stiffness before failing.



**Figure 7:** Stiffness degradation versus number of cycles.

The maximum CMOD is seen to gradually rise in Figure 8, which corresponds to the A3 specimen, demonstrating that the damage is of a permanent nature without any recovery, which is quite typical of a quasi-brittle material. In the beginning, as the load is applied, it is seen that CMOD grows quickly as a result of the formation of distributed microcracks in the sample ahead of the notch. However, when the number of fatigue cycles rises, a steady rise in CMOD is seen, indicating that more and more microcracking is occurring. The value of CMOD increases exponentially close to the test sample failure point, as microcracks combine to form macro-crack that cause the specimen to fail.



**Figure 8:** Maximum CMOD versus number of cycles.

### 3.2 Acoustic Emission Results

The present research used the AE method to track the development of microcracks brought on by fatigue loading. The AE events qualitatively show that the material has developed microcracks.

From Figure 9, the AE events which represent micro cracks in fatigue loading appears to be scattered throughout the specimen and not concentrated near the notch as seen in monotonic loading. Microcracks that develop in the specimen throughout the course of fatigue life cause the material's stiffness to gradually deteriorate until a critical stiffness is reached, beyond which failure occurs suddenly with macrocrack propagation occurring only during the final load cycle.

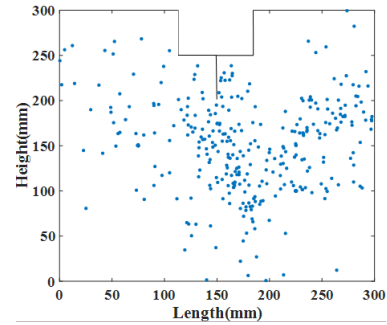


**Figure 9:** Location of AE events (At Failure)

Cumulative number of AE events and cumulative absolute AE energy is displayed against time for a 50 mm notch specimen in Figure 10 and Figure 11 respectively, which corresponds to the A4 specimen. Both the plots have a similar trend. It is seen that in the initial part of fatigue life there is a low rate of increase in the number of AE events and absolute AE energy, since the microcracks generated have low absolute AE energy. These low-energy, brief jumps could be the result of cement mortar failure. The absolute AE energy produced during subsequent cycles of the fatigue load accumulates, and the rate of growth in energy accelerates as a result of the coalescence of microcracks into macrocracks. It can be seen that the increase in AE events and absolute AE energy have a nearly linear pattern over the majority of its fatigue life before rising suddenly just before failure. The aggregate slip or breaking at the specimen's final cycle of failure may be responsible for the greater energy jumps.

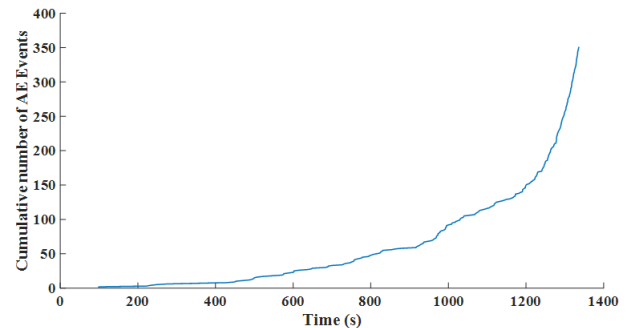


**Figure 10:** Cumulative number of events versus time.

Figure 11 also depicts the occurrence of AE

events of various energies over time for a specimen that was subjected to fatigue loading. The initial warming cycles in the graph contain a few low-level AE events. It means that a very small number of low energy microcracks start to form inside the specimen as soon as the loading is applied. A few AE events from all energy levels are seen throughout the test, up until failure. It may be argued that during fatigue loading, the major cracks form near failure, causing an abrupt failure. At the time of failure, a significant number of AE events occur. There are more AE events with lower energy levels. Furthermore, the lack of high-energy AE events supports the notion that fracture propagation only occurs in the last cycle. This might be because the macrocrack at the point of failure propagates so quickly that the AE sensors are unable to capture it.

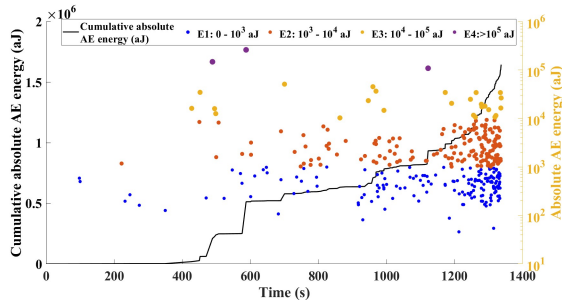


**Figure 11:** Distribution of events based on AE energy

RA-AF analysis as performed in [9] is used to determine the percentage of tensile cracks that develop in the specimen under fatigue loading. The table shows that tensile cracks account for more than 99% of all cracks. The RA-AF plot is shown in Figure 12, with the majority of AE occurrences occurring in the tensile area. Table 2 represents the number of events to failure, cumulative absolute AE energy and the results of RA-AF analysis performed. FPZ with the typical definition is not formed in concrete as an isolated and randomly distributed micro cracks are formed under fatigue loading, according to results from these experiments.

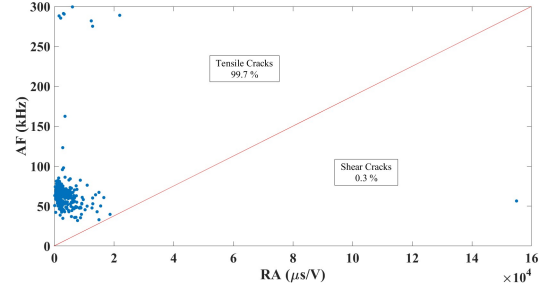


**Figure 12:** RA-AF analysis.

**Table 2:** AE test results for fatigue loading.

ID	Number of Events at failure	Cumulative absolute AE energy ( $10^6 a.J$ )	Tensile cracks (RA-AF)
A2	335	3.488	99.11
A3	330	7.296	99.7
A4	351	1.644	100

## 4 CONCLUSIONS

In the current research, wedge splitting specimens are used to conduct an experimental investigation on the impact of constant amplitude fatigue loading in concrete. The micro-cracking mechanisms in concrete are measured using the acoustic emission technique. The experiments conducted led to the conclusions that are given below.

- Results indicate that the stiffness of the specimens decrease from the beginning of the load application till failure. The stiffness decrease with the load cycles is observed to have three distinctive zones. In the first zone, a decrease in stiffness is observed as the specimen is loaded. In the second zone, a steady rate of stiffness degradation is observed. In the third zone, due to the coalescing of the internal micro cracks, a sudden decrease in stiffness is observed as the crack becomes unstable leading to failure.
- With repeated loading cycles, concrete is found to suffer progressive deterioration

and an increase in CMOD value. During the fatigue process, microcracks start to form and gradually merge together to produce larger cracks, causing damage. For the majority of the fatigue life, a consistent rate of increase in the maximum CMOD value is seen.

- According to the distribution of AE events over time and their locations inside the specimen, the formation of microcracks occurs randomly across the specimen for up to 75–80% of the fatigue life. The number of AE events increases exponentially when approaching the final cycles of failure, wherein the microcracks combines to form a macrocrack and it propagates only in the final cycle of the fatigue life.
- Reliable proof has been provided by the studies that FPZ, as it is typically defined, does not appear in concrete as a result of fatigue loading since isolated and randomly oriented microcracks are formed throughout the test.

## REFERENCES

- [1] Subramaniam V. Kolluru, Edward F. O’Neil, John S. Popovics, and Surendra P. Shah. 2000. Crack Propagation in Flexural Fatigue of Concrete. *Journal of Engineering Mechanics*. 126(9), pp. 891-898.
- [2] Jianzhuang Xiao, Holger Schneider, Cindy Donnecke, and Gert Konig. 2004. Wedge splitting test on fracture behaviour of ultra-high strength concrete. *Construction and Building Materials*. 18, pp. 359–365.
- [3] Li-Ping Guo, Wei Sun, Xiao-Yuan He, and Zhen-Bin Xu. 2008. Application of DSCM in prediction of potential fatigue crack path on concrete surface. *Engineering Fracture Mechanics*. 75, pp. 643–651.
- [4] I. Lofgren, H. Stang, and J. F. Olesen. 2008. The WST method, a fracture mechanics test method for FRC. *Materials and Structures*. 41, pp. 197-211.
- [5] Santosh G. Shah and J.M. Chandra Kishen. 2012. Use of acoustic emissions in flexural fatigue crack growth studies on concrete. *Engineering Fracture Mechanics*. 87, pp. 36-47.
- [6] Marta Sitek, Grzegorz Adamczewski, Marcin Szyszko, Bartóomiej Migacz, Paweá Tutka, and Maja Natorff. 2014. Numerical Simulations of a Wedge Splitting Test for High-Strength Concrete. *Procedia Engineering*. 91, pp. 99-104.
- [7] K. Keerthana and J.M. Chandra Kishen. 2018. An experimental and analytical study on fatigue damage in concrete under variable amplitude loading. *International Journal of Fatigue*. 111, pp. 278-288.
- [8] ] K. Keerthana and J.M. Chandra Kishen. 2020. Micromechanics of fracture and failure in concrete under monotonic and fatigue loadings. *Mechanics of Materials*. 148, 103490.
- [9] Parvinder Singh, R. Yogesh, Sonali Bhowmik, J. M. Chandra Kishen. 2023. Insights into the fracturing process of plain concrete under crack opening. *International Journal of Fracture*. 241, pp. 153-170.